APPLIED PHYSICS LETTERS **105**, 083901 (2014)

Development of bulk-type all-solid-state lithium-sulfur battery using $LiBH_4$ electrolyte

Atsushi Unemoto,[1,a)] Syun Yasaku,[2] Genki Nogami,[3] Masaru Tazawa,[3] Mitsugu Taniguchi,[3]
Motoaki Matsuo,[2] Tamio Ikeshoji,[1] and Shin-ichi Orimo[1,2]
[1]*WPI-Advanced Institute for Materials Research, Tohoku University, 2-1-1 Katahira, Aoba-ku, Sendai 980-8577, Japan*
[2]*Institute for Materials Research, Tohoku University, 2-1-1 Katahira, Aoba-ku, Sendai 980-8577, Japan*
[3]*Mitsubishi Gas Chemicals Co., Ltd., 182 Tayuhama Shinwari, Kita-ku, Niigata 950-3112, Japan*

(Received 15 July 2014; accepted 8 August 2014; published online 25 August 2014)

Stable battery operation of a bulk-type all-solid-state lithium-sulfur battery was demonstrated by using a $LiBH_4$ electrolyte. The electrochemical activity of insulating elemental sulfur as the positive electrode was enhanced by the mutual dispersion of elemental sulfur and carbon in the composite powders. Subsequently, a tight interface between the sulfur-carbon composite and the $LiBH_4$ powders was manifested only by cold-pressing owing to the highly deformable nature of the $LiBH_4$ electrolyte. The high reducing ability of $LiBH_4$ allows using the use of a Li negative electrode that enhances the energy density. The results demonstrate the interface modification of insulating sulfur and the architecture of an all-solid-state Li-S battery configuration with high energy density. © *2014 AIP Publishing LLC*. [http://dx.doi.org/10.1063/1.4893666]

Lithium-sulfur (Li-S) rechargeable batteries are expected to act as next generation energy reservoirs for large-scale applications including vehicles and stationary uses. The electrochemical reaction of the S/Li redox couple, $2Li^+ + 2e^- + S \rightleftarrows Li_2S$, has high capacity (1672 mA h g^{-1} at an average redox potential of 2.2 V *vs.* Li/Li$^+$), resulting in a high energy density (∼2600 W h kg^{-1} versus ∼400 W h kg^{-1} for a commercial $LiCoO_2$/C cell).[1–4]

A major technological challenge in assembling Li-S rechargeable batteries is developing the electrolytes that ensure stable operation and enhance the sulfur utilization ratio.[1–4] Among the liquid electrolytes, though ethers are considered as possible candidate solvents, they readily solubilize the reduced products, i.e., the lithium polysulfides.[5] Such dissolution of lithium polysulfides accelerates loss of the active materials, redox shuttling (which lowers the coulombic efficiency), and corrosion of the Li negative electrode. All of these processes destabilize the battery operation.[1–4] Another candidate for the liquid electrolyte is room temperature ionic liquids (RTILs).[6–12] Although lithium polysulfides are relatively insoluble in RTILs, the power density and sulfur utilization ratio are both limited by the slow Li ion diffusivity in these liquids.[11,13,14] Hence, electrolytes that prevent the dissolution of lithium polysulfides into the electrolyte while ensuring high Li-ionic conductivity are urgently required.

Recognizing that these criteria are fulfilled by sulfide-based solid electrolytes, researchers have recently assembled stable bulk-type all-solid-state Li-S batteries.[15–19] Sulfide-based solid-state electrolytes generally require Li alloy negative electrodes with higher potential than the Li negative electrode (e.g., the potentials of LiIn and $Li_{38}Al_{68}$ are 0.62 and 0.38 V, respectively, *vs.* Li/Li$^+$ at 297 K). Use of such alloy negative electrodes lowers cell voltage, and thereby compromising the energy density. Therefore, the success of the bulk-type all-solid-state Li-S batteries relies on developing solid-state electrolytes that not only possess high Li-ionic conductivity but are also electrochemically compatible with the Li negative electrode.

Complex hydride-based fast Li-ionic conductors, typically the high-temperature phase of $LiBH_4$ (S.G.: $P6_3mc$),[20] may overcome the aforementioned technological issues.[21] Above 390 K, the Li-ionic conductivity of $LiBH_4$ exceeds 2×10^{-3} S cm^{-1}. This high conductivity is accompanied by a structural transition from orthorhombic to hexagonal systems at elevated temperatures.[22,23] The fast Li-ionic conduction is realized by intrinsically induced mobile ionic defects, and subsequent Li-site percolation with low activation energy for Li migration.[24–26] The strong reducing ability of the materials confers high electrochemical compatibility to the Li negative electrode.[21–23] The complex hydrides possess attractive mechanical properties that assist the rechargeable battery assemblies. The highly deformable nature of the complex hydrides enables compact preparation approaching the theoretical density. A tight interface between the active materials and electrolyte particles can be realized merely by uniaxial pressing at room temperature. The close attachment between the active material and the electrolyte phases establishes an interface that allows charge transfer three-dimensionally in the composite electrodes, enhancing the positive electrode utilization ratio.[21] Therefore, complex hydride electrolytes are valuable components of the bulk-type all-solid-state Li-S battery assembly.

In this work, we report the development of a bulk-type all-solid-state Li-S rechargeable battery using the fast Li-ion conducting $LiBH_4$ electrolyte. Because the interface among the sulfur, conductive additive, and $LiBH_4$ allows charge transfer three-dimensionally in the composite positive electrode, the battery achieves a stable discharge-charge cycle performance with a high sulfur utilization ratio. The energy density of the battery is enhanced by the high electrochemical compatibility of the $LiBH_4$ electrolyte to the Li negative electrode.

[a)] Electronic mail: unemoto@imr.tohoku.ac.jp

© 2014 AIP Publishing LLC

The insulating elemental sulfur must be effectively dispersed along the conductive additive surfaces to improve its electrochemical activity.[1–4] In this study, we prepared S-C composites by the high-energy mechanical ball milling process.[15–19] The conductive additives were Ketjen Black (KB), activated carbon, Maxsorb®, and a KB-Maxsorb® mixture (1:1 in wt.).[27] Being more electronically conductive than Maxsorb, KB increases the electronic conductivity of the composite. In contrast, Maxsorb has a larger specific surface area than KB, and it increases the concentration of the sulfur-Maxsorb interface. The mixed conductive additive is expected to enhance both the S-C interface concentration and the electronic conductivity, thus enhancing the electrochemical activity of the insulating elemental sulfur.

To examine the microstructure of the S-C composite powder as a result of the high-energy mechanical ball milling at 400 rpm for 20 h, a S-KB-Maxsorb/$LiBH_4$ compact was prepared by cold pressing at 240 MPa. Subsequently, the cross-section was prepared by using a focused ion beam with a Ga-ion radiation. Figure 1 shows the cross-sectional images of the S-KB-Maxsorb/$LiBH_4$ compact observed by a field emission scanning electron microscopy (FE-SEM) and bright-field scanning transmission electron microscopy (BF-STEM). Carbon and sulfur distributions were also analyzed by an energy dispersive X-ray spectrometer (EDS).[27] The figure confirms the dispersal of sulfur and carbon in the powdered S-C composite. The Brunauer-Emmett-Teller (BET) specific surface areas, S_{BET}, of the S-C powdered products were analyzed from nitrogen adsorption-desorption isotherms obtained at 77 K. S_{BET} was below 1 $m^2\ g^{-1}$ regardless of the conductive additive species (3083 $m^2\ g^{-1}$, 2126 $m^2\ g^{-1}$, and 1345 $m^2\ g^{-1}$ for Maxsorb, KB-Maxsorb, and KB, respectively), suggesting that carbon particles are essentially confined within the powder products. As a result of high and mutual dispersion of carbon and sulfur inside the powders, a large area of the S-C interface was exposed to the particle surfaces. The microstructure is advantageous in that it facilitates the development of an interface that allows the smooth charge transfer with the $LiBH_4$ electrolyte.

Although the S-KB-Maxsorb/$LiBH_4$ compact was prepared by cold pressing, the deformable S-C and $LiBH_4$ particles ensured that the S-KB-Maxsorb composite and $LiBH_4$ phases were closely attached in the S-KB-Maxsorb/$LiBH_4$ layer as shown in Figs. 1(a) and 1(b). Although annealing at the battery operating temperature, i.e., 393 K, for 3 h in an Ar-filled environment introduced small morphological changes in the S-KB-Maxsorb/$LiBH_4$ composite positive electrode, the concentration of the interface between S-KB-Maxsorb and $LiBH_4$ remain high as displayed in Figs. 1(e) and 1(f). The high mutual dispersion of the mixed KB and Maxsorb conductive additive and the subsequent introduction of the $LiBH_4$ phase were responsible for the formation of an interface that allows smooth charge transfer in the composite positive electrode. Microstructural changes of the S-KBMaxsorb/$LiBH_4$ compact accompanied by gas desorption was limited to the beginning of the annealing.[27] Therefore, the composite positive electrode microstructure achieved a stable bulk-type all-solid-state Li-S rechargeable battery at 393 K.

Figure 2(a) shows typical discharge-charge profiles of the S-KB-Maxsorb/$LiBH_4$ | $LiBH_4$ | Li rechargeable cells operated at 0.05 C (corresponding to a current density of $\sim$250 μA cm^{-2}). The initial discharge capacity was 1140 mA h g^{-1} (70% sulfur utilization ratio), exceeding that of the S-KB/$LiBH_4$ | $LiBH_4$ | Li cell (950 mA h g^{-1} operated at a lower C-rate, 0.02 C).[27] The S-Maxsorb/$LiBH_4$ | $LiBH_4$ | Li rechargeable cell exhibited a lower sulfur utilization ratio and reduced cycle life even though the microstructure of the S-Maxsorb powder was very similar to that of the other S-C powders.[27] The poorer performance of the cell using Maxsorb as a conductive additive is attributed to the low electronic conductivity of Maxsorb. The mixed KB and Maxsorb conductive additive increased both the interface concentration and the electronic conductivity. Hence, a high sulfur utilization ratio was realized owing to the enhanced electrochemical activity of the S-C powder product. Figure 2(b) shows the discharge capacity and the coulombic efficiency as a function of cycle numbers. The 45th discharge capacity remains as high as 730 mA h g^{-1} with nearly 100% coulombic efficiency over the discharge-charge cycles. The results suggest that our composite positive electrode realized the stable interface formation among the elemental sulfur, mixed conductive additive, and $LiBH_4$ without any side reactions during the battery operation.

Our bulk-type all-solid-state cell also exhibited notable high-rate performance. Figure 3 shows the discharge profiles at 0.05–1 C for discharge. Even at the higher discharge rate of 0.5 C (corresponding to 2.5 mA cm^{-2}), our bulk-type

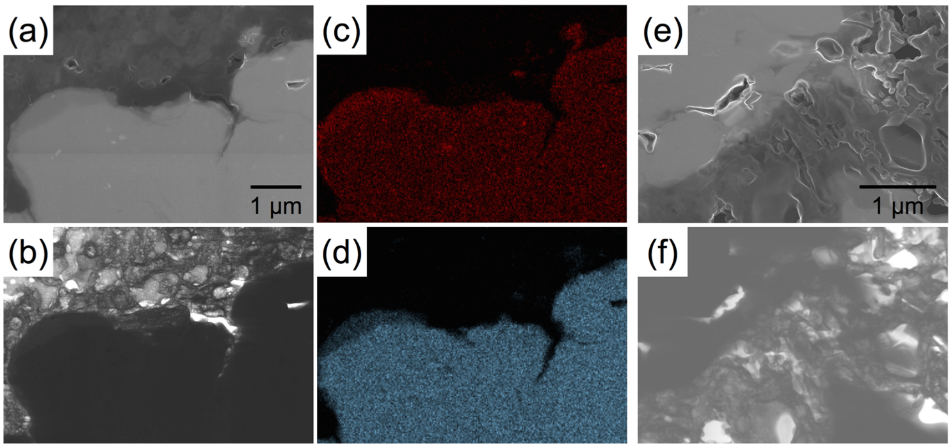

FIG. 1. Cross-sectional (a) FE-SEM and (b) BF-STEM images, and element distributions of (c) carbon and (d) sulfur in the as-prepared S-KB-Maxsorb/$LiBH_4$ compact. Cross-sectional (e) FE-SEM and (f) BF-STEM images of the S-KB-Maxsorb/$LiBH_4$ compact after annealing at 393 K for 2 h in an Ar-filled environment.

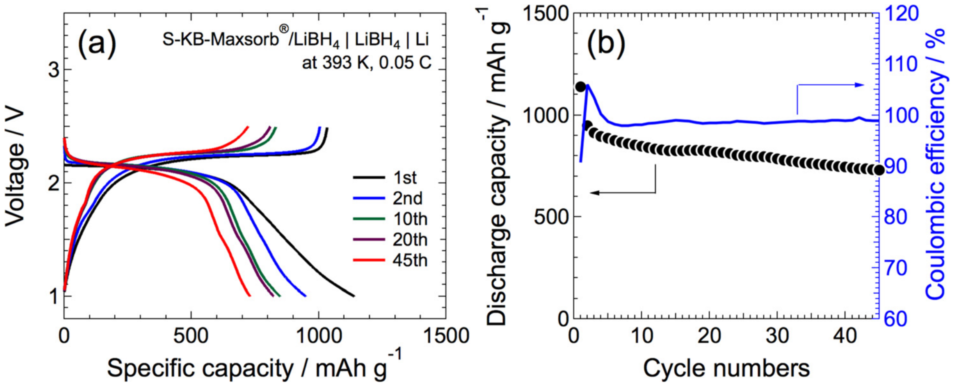

FIG. 2. (a) Typical discharge-charge profiles of the S-KB-Maxsorb/$LiBH_4$|$LiBH_4$|Li rechargeable cell operated at 393 K and 0.05 C. (b) Discharge capacity and the coulombic efficiency as a function of cycle numbers.

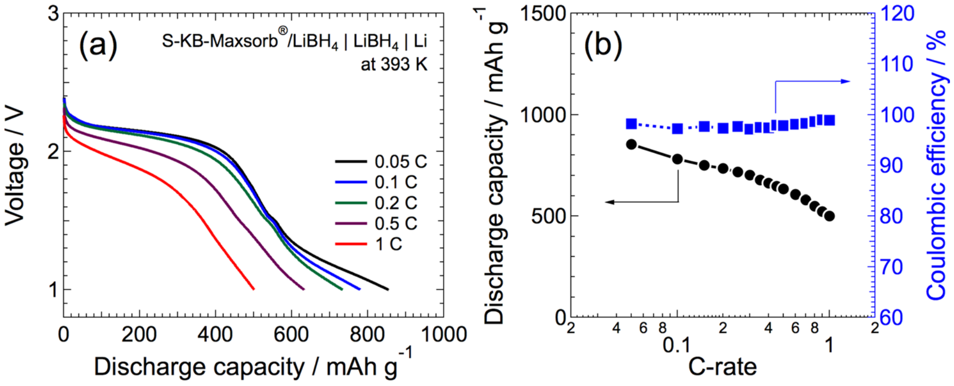

FIG. 3. (a) Representative discharge profiles of the S-KB-Maxsorb/$LiBH_4$|$LiBH_4$|Li rechargeable cell operated at 393 K and 0.05–1 C. Considering the capacity fade in the initial few cycles, the battery was operated at 0.05 C for three cycles: the C-rate was then increased to 1 C. Charge was carried out at 0.05 C regardless of the discharge rate. (b) Discharge capacity and the coulombic efficiency as a function of the C-rate.

all-solid-state Li-S battery retained a discharge capacity of 630 mA h g^{-1}. The energy density of our battery was calculated to be 1110 W h kg^{-1} on the basis of the relationship between the voltage and the discharge capacity. It should be noted that both a high sulfur utilization ratio and high voltage by the use of the Li negative electrode are responsible for enhancing the energy density of the rechargeable battery. The discharge capacities were always smaller than their theoretical values (1672 mA h g^{-1}), and they monotonically decreased with increasing discharge rate. This implies that slow electrochemical reduction is the rate-limiting process, especially at the end of the discharge where Li_2S is formed, as observed in the non-aqueous systems.[3,4,8–12] Currently, we are systematically investigating the high-rate performance with an asymmetric operations for charge and discharge. As a result, the electrochemical oxidation of Li_2S was found to be slower than the electrochemical reduction of S (data not shown). On the basis of this finding, we are further optimizing the composite positive electrode structure and the composition that will further enhance energy and power densities.

In summary, we have demonstrated the stable battery operation of a bulk-type all-solid-state Li-S rechargeable battery using a $LiBH_4$ electrolyte and a Li negative electrode. The energy density and cycle life were enhanced by high-energy mechanical ball milling, which properly disperses the elemental sulfur and the mixed conductive additives, KB and Maxsorb. Equally important is the high deformability of the complex hydrides, which ensures a tight interface between the S-C and $LiBH_4$ phases. These result in the formation of the high concentration of the stable interface that allows smooth charge transfer three-dimensionally across the composite positive electrode layer among the sulfur, mixed conductive additive, and $LiBH_4$. By incorporating the complex hydride-based solid-state electrolytes in the bulk-type all-solid-state Li-S battery, we realized a battery design that will ensure a high energy density. Use of complex hydride-based solid-state electrolytes that exhibit the fast Li-ionic conduction at reduced temperatures, namely, $LiBH_4$-$LiNH_2$-LiI,[28,29] $LiRE(BH_4)_3Cl$ (RE = Ce, La, and Gd),[30,31] and Li_3AlH_6,[32] would be beneficial to lower the battery operating temperature. Based on the proposed device concept, the use of complex hydrides that allow fast ionic conduction of abundant and cost-effective species, such as Na[33–35] and Mg,[36] are also expected to become integrated into high energy density rechargeable batteries.

The authors would like to thank Mr. K. Sato, Ms. H. Ohmiya, and Ms. N. Warifune for technical assistance. Financial support from the Target Project 4 of WPI-AIMR, Tohoku University, the Integrated Materials Research Center for the Low-Carbon Society (LC-IMR), Tohoku University, JSPS KAKENHI Grant No. 25220911, and the Advanced Low Carbon Technology Research and Development Program (ALCA) from the Japan Science and Technology Agency (JST) are gratefully acknowledged.

[1] P. G. Bruce, S. A. Freunberger, L. J. Hardwick, and J.-M. Tarascon, Nat. Mater. **11**, 19 (2012).
[2] X. Ji and L. F. Nazar, J. Mater. Chem. **20**, 9821 (2010).
[3] Y.-X. Yin, S. Xin, Y.-G. Guo, and L.-J. Wan, Angew. Chem. Int. Ed. **52**, 13186 (2013).
[4] S. S. Zhang, J. Power Sources **231**, 153 (2013).
[5] J. Gao, M. A. Lowe, Y. Kita, and H. D. Abruna, J. Phys. Chem. C **115**, 25132 (2011).

[6] L. X. Yuan, J. K. Feng, X. P. Ai, Y. L. Cao, S. L. Chen, and H. X. Yang, Electrochem. Commun. **8**, 610 (2006).

[7] J. Wang, S. Y. Chew, Z. W. Zhao, S. Ashraf, D. Wexler, J. Chen, S. H. Ng, S. L. Chou, and H. K. Liu, Carbon **46**, 229 (2008).

[8] N. Tachikawa, K. Yamauchi, E. Takashima, J.-W. Park, K. Dokko, and M. Watanabe, Chem. Commun. **47**, 8157 (2011).

[9] H. Ogawa, A. Unemoto, and I. Honma, Electrochemistry **80**, 765 (2012).

[10] J.-W. Park, K. Yamauchi, E. Takashima, N. Tachikawa, K. Ueno, K. Dokko, and M. Watanabe, J. Phys. Chem. C **117**, 4431 (2013).

[11] K. Dokko, N. Tachikawa, K. Yamauchi, M. Tsuchiya, A. Yamazaki, E. Takashima, J.-W. Park, K. Ueno, S. Seki, N. Serizawa, and M. Watanabe, J. Electrochem. Soc. **160**, A1304 (2013).

[12] A. Unemoto, H. Ogawa, Y. Gambe, and I. Honma, Electrochim. Acta **125**, 386 (2014).

[13] H. Matsumoto, H. Sakaebe, K. Tatsumi, M. Kikuta, E. Ishiko, and M. Kono, J. Power Sources **160**, 1308 (2006).

[14] A. Unemoto, H. Ogawa, S. Ito, and I. Honma, J. Electrochem. Soc. **160**, A138 (2013).

[15] T. Kobayashi, Y. Imade, D. Shishihara, K. Homma, M. Nagao, R. Watanabe, T. Yokoi, A. Yamada, R. Kanno, and T. Tatsumi, J. Power Sources **182**, 621 (2008).

[16] M. Nagao, A. Hayashi, and M. Tatsumisago, Electrochim. Acta **56**, 6055 (2011).

[17] M. Nagao, A. Hayashi, and M. Tatsumisago, Electrochem. Commun. **22**, 177 (2012).

[18] M. Nagao, Y. Imade, H. Narisawa, T. Kobayashi, R. Watanabe, T. Yokoi, T. Tatsumi, and R. Kanno, J. Power Sources **222**, 237 (2013).

[19] M. Nagao, Y. Imade, H. Narisawa, R. Watanabe, T. Yokoi, T. Tatsumi, and R. Kanno, J. Power Sources **243**, 60 (2013).

[20] S. Orimo, Y. Nakamori, J. R. Eliseo, A. Züttel, and C. M. Jensen, Chem. Rev. **107**, 4111 (2007).

[21] A. Unemoto, M. Matsuo, and S. Orimo, Adv. Funct. Mater. **24**, 2267 (2014).

[22] M. Matsuo, Y. Nakamori, S. Orimo, H. Maekawa, and H. Takamura, Appl. Phys. Lett. **91**, 224103 (2007).

[23] M. Matsuo and S. Orimo, Adv. Energy Mater. **1**, 161 (2011).

[24] T. Ikeshoji, E. Tsuchida, K. Ikeda, M. Matsuo, H.-W. Li, Y. Kawazoe, and S. Orimo, Appl. Phys. Lett. **95**, 221901 (2009).

[25] T. Ikeshoji, E. Tsuchida, T. Morishita, K. Ikeda, M. Matsuo, Y. Kawazoe, and S. Orimo, Phys. Rev. B **83**, 144301 (2011).

[26] J. S. G. Myrdal, D. Blanchard, D. Sveinbjörnsson, and T. Vegge, J. Phys. Chem. C **117**, 9084 (2013).

[27] See supplementary material at http://dx.doi.org/10.1063/1.4893666 for the experimental setup, the characterizations of the specimens, and the results of battery tests.

[28] H. Maekawa, M. Matsuo, H. Takamura, M. Ando, Y. Noda, T. Karahashi, and S. Orimo, J. Am. Chem. Soc. **131**, 894 (2009).

[29] M. Matsuo, A. Remhof, P. Martelli, R. Caputo, M. Ernst, Y. Miura, T. Sato, H. Oguchi, H. Maekawa, H. Takamura, A. Borgshulte, A. Züttel, and S. Orimo, J. Am. Chem. Soc. **131**, 16389 (2009).

[30] M. B. Ley, D. B. Ravnsbaek, Y. Filinchuk, Y.-S. Lee, R. Janot, Y. W. Cho, J. Skibsted, and T. R. Jensen, Chem. Mater. **24**, 1654 (2012).

[31] M. B. Ley, S. Boulineau, R. Janot, Y. Filinchuk, and T. R. Jensen, J. Phys. Chem. C **116**, 21267 (2012).

[32] H. Oguchi, M. Matsuo, T. Sato, H. Takamura, H. Maekawa, H. Kuwano, and S. Orimo, J. Appl. Phys. **107**, 096104 (2010).

[33] M. Matsuo, S. Kuromoto, T. Sato, H. Oguchi, H. Takamura, and S. Orimo, Appl. Phys. Lett. **100**, 203904 (2012).

[34] H. Oguchi, M. Matsuo, S. Kuromoto, H. Kuwano, and S. Orimo, J. Appl. Phys. **111**, 036102 (2012).

[35] T. J. Udovic, M. Matsuo, A. Unemoto, N. Verdal, V. Stavila, A. V. Skripov, J. J. Rush, H. Takamura, and S. Orimo, Chem. Commun. **50**, 3750 (2014).

[36] S. Higashi, K. Miwa, M. Aoki, and K. Takechi, Chem. Commun. **50**, 1320 (2014).

Applied Physics Letters is copyrighted by the American Institute of Physics (AIP). Redistribution of journal material is subject to the AIP online journal license and/or AIP copyright. For more information, see http://ojps.aip.org/aplo/aplcr.jsp